SHIELDING AND MAGNIFICATION OF LOADS IN ELASTIC, UNIDIRECTIONAL COMPOSITES

A.M. Sastry

Sibley School of Mechanical and Aerospace Engineering, Cornell University, Ithaca, New York

S.L. Phoenix

Theoretical and Applied Mechanics, Cornell University, Ithaca, New York

ABSTRACT

The strength of composite materials exhibits a scale effect, and computationally efficient schemes are required for performing large simulations to characterize the relationship between strength distributions and size in composites, incorporating both the statistical and mechanical aspects of the problem. A new technique for calculating load profiles in unidirectional, elastic composites containing arbitrarily located breaks is used to demonstrate magnification and shielding effects among breaks in the planar setting, which profoundly influence break (crack) progression and ultimate strength distributions. Three-dimensional solution techniques are also outlined.

INTRODUCTION

The strength of fibrous composite materials is determined by the strength distribution of the reinforcing fibers and the mechanics of load redistribution around fiber breaks. The strength of these brittle fibers, unlike the strength of ductile engineering materials such as metals, exhibits a scale effect: that is, long fibers are weaker than short fibers. This scale effect has been observed by many workers [(1-3) for example]. The scale effect results from the mechanism of tensile failure of the fibers. Brittle fibers are generally strong and uniform in diameter, but contain a distribution of flaws of different strength which cause failure, and one is more likely to find a flaw in a longer fiber than in a short fiber. As a result of this scale effect in reinforcing fibers, it has been argued that large composites are generally weaker than small composites (4-6).

There is a substantial body of work available regarding the purely statistical aspects of the problem of scale effect in strength in fiber structures. Daniels' bundle strength work (7), in which the strength of large, dry bundles using the statistics of the constituent fibers was derived, is the classic work in this area; it has been incorporated into analyses for structures from twisted and braided ropes to composite materials (for a review, see Reference 8).

In composite materials containing broken fibers, however, the load sharing becomes much more complicated by the presence of the matrix. The details of this load transfer between broken and unbroken fibers are, in fact, critical in predicting composite strength. Work has been carried out using both simple load sharing rules to approximate mechanical behavior in a composite (9-10) and incorporating the micromechanics of load transfer (11-12). Each of these techniques has inherent problems. The former, purely statistical approaches, while mathematically more tractable, overly idealize the mechanical load transfer occurring in the real composite, which can produce substantially different overloads on unbroken fibers than simple mathematical rules would impose, particularly in the case of clustered breaks. In the latter, micromechanical approaches, finite difference or finite element methods are used to account for the more complicated load sharing. As a result, many types of interfacial and matrix constitutive behaviors can be modeled, but the simulations are limited by the amount of computation required, and simulations of sizes of composites of interest to designers (10^6 multiples of fiber diameters) quickly become impractical.

ANALYSIS: THE BIS TECHNIQUE

In the shear-lag model used in the present work, a superposition technique for calculating stresses in cracked solids developed by Kachanov (13-14) for isotropic materials is modified for use in unidirectional composites. This model, the break-influence superposition (BIS) technique, is an improvement to Hedgepeth's analyses (15). In this analysis, and in modifications to it (16-17), stress profiles in infinite composites containing breaks along a single transverse line (perpendicular to the fibers' axes) were calculated. Using the present technique, fiber load profiles can be found for composites containing arbitrarily located breaks, as would occur in a real composite. The BIS also offers an important advantage over the micromechanical analysis techniques above in terms of speed of computation in the purely elastic load-transfer case.

The technique consists of three calculations. First, the solution for the overloads in an infinite, unidirectional, fully elastic composite sheet containing a single fiber break is obtained using Hedgepeth's shear-lag technique. Then, interactions among arbitrarily located breaks are found, and using boundary conditions forcing the load to negative unity at the break sites, a superposition technique is used to solve for the over-

loads in the sheet with many breaks. Finally, a unit load is added to the fiber load solution, resulting in zero loads at each break site, and unit (applied) edge loads parallel to the fibers at infinity. This yields overload factors for all fiber points in the composite. Figure 1a shows a schematic of Hedgepeth's notation, which is adopted here for the multiple break problem, and Figure 1b shows a free body diagram of a fiber element in fiber n. In Hedgepeth-type approaches (15-17), fiber breaks were assumed to occur only along a single transverse line, at $\xi = 0$ (see Figure 1a).

By shear-lag assumptions, the derivative of normal fiber load with axial position is proportional to matrix shear stress. The governing equation is written in terms of normalized displacements as

$$\frac{\partial^2 U_n}{\partial \xi^2} + U_{n+1} - 2U_n + U_{n-1} = 0 \qquad [1]$$

where the normalized fiber constitutive equation, fiber load, fiber axial displacement, and axial position (for fiber n) are

$$P_n = \frac{\partial U_n}{\partial \xi}, \qquad [2]$$

$$P_n = \frac{p_n}{p}, \qquad [3]$$

$$U_n = \frac{u_n}{p\sqrt{\frac{b}{EAGh}}}, \qquad [4]$$

and

$$\xi = \frac{x}{\sqrt{\frac{EAb}{Gh}}} \qquad [5]$$

respectively, and the actual fiber load, fiber displacement and axial position are P_n, u_n, and x, respectively. The variables p, A, G, and E are the applied edge load per fiber, fiber cross-sectional area ($A = b \bullet h$), matrix shear modulus and fiber Young's modulus, respectively. The normalizations of Equations 3 and 4, although unintuitive to say the least, simplify calculations by allowing the convenient normalizations of Equations 1 and 2.

The details of the technique are described in Reference 18, an outline of the technique follows. The final load distribution for a composite with fiber break positions (n_1, ξ_1), (n_2, ξ_2), (n_3, ξ_3), etc. is given by

$$P_n(\xi) = K_1 F_{n-n_1}(\xi - \xi_1) + K_2 F_{n-n_2}(\xi - \xi_2) + K_3 F_{n-n_3}(\xi - \xi_3) + \ldots + 1, \qquad [6]$$

where the same fiber may have several breaks along its axis ($n_2 = n_3$, for example), or several fibers have breaks at the same axial location ($\xi_1 = \xi_2 = \xi_3$, for example).

The individual breaks' solutions, for zero edge load and negative unit tensile load at the broken fiber ends, are

$$F_{n-n_i}(\xi - \xi_i) = \frac{-1}{2}\int_0^{\pi} \sin\left(\frac{\theta}{2}\right)\cos([n-n_i]\theta)\, e^{-2|\xi-\xi_i|\sin\frac{\theta}{2}}\, d\theta \qquad [7]$$

and the boundary conditions are given by (for a sample case of three breaks)

$$\begin{Bmatrix} -1 \\ -1 \\ -1 \end{Bmatrix} = \begin{bmatrix} A_{11} & A_{12} & A_{13} \\ A_{12} & A_{22} & A_{23} \\ A_{13} & A_{23} & A_{33} \end{bmatrix} \begin{Bmatrix} K_1 \\ K_2 \\ K_3 \end{Bmatrix}, \qquad [8]$$

where the transmission factors A_{ij} are

$$A_{ij} = \frac{-1}{2}\int_0^{\pi} \sin\left(\frac{\theta}{2}\right)\cos([n_i - n_j]\theta)\, e^{-2|\xi_i-\xi_j|\sin\frac{\theta}{2}}\, d\theta \qquad [9]$$

Using this technique, the single-break problem needs to be solved only once for loads on a fine grid of points along overloaded fibers; shifting of this solution to obtain solutions

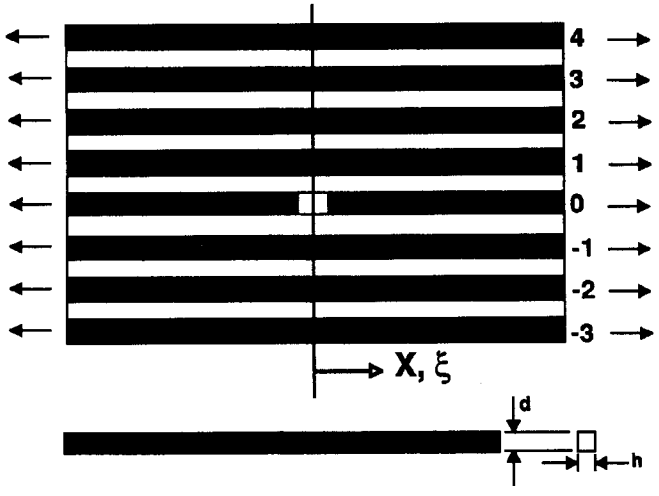

(a)

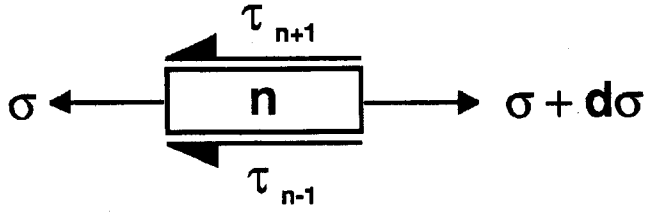

(b)

Figure 1. a) Schematic of the problem solved by Hedgepeth (5) with notation, and b) Free-body diagram of an element of fiber n.

to Equations 7 and 9, and solution of boundary conditions such as those in Equation 8 can then be used to solve the multiple break problem. The amount of computation is thus tied to the number of breaks. The amount of computation in the finite difference and finite element solutions, by contrast, is tied to the total volume of the composite.

Only the loads in a quarter of the plane shown in Fig. 1 ($\xi \geq 0$, $n \geq 0$) must be found for the single-break problem because of its symmetry. These loads are found through numerical integration of Equation 7. Also, because the loads return to one at some distance away from a break, solution of the single break problem is only required for about 15 fibers, and for an axial length of about $\xi = 16$, at which points the loads have returned to within 0.001 of the unit load.

MAGNIFICATIONS OF LOADS WITH MULTIPLE BREAKS

Figures 2 and 3 show the load profiles on nearby fibers for one break and two aligned breaks, respectively. These problems are of the type solved by Hedgepeth. Figure 4a shows how tensile load on a broken fiber builds axially, away from the break, while Figure 4b shows how the tensile loads in the fibers adjacent to aligned broken fibers vary axially. The tensile loads in broken fibers in the case of two breaks require a longer axial length to reach the edge unit load, as is shown in Figure 4a, and the neighboring fibers to the broken fibers are more highly overloaded in the case of two breaks than in the case of a single break, as can be seen by Figure 4b, and comparison of Figures 1 and 2. The overload on the adjacent fiber to a broken fiber occurs over an axial length that is on the order of $\xi = 1$.

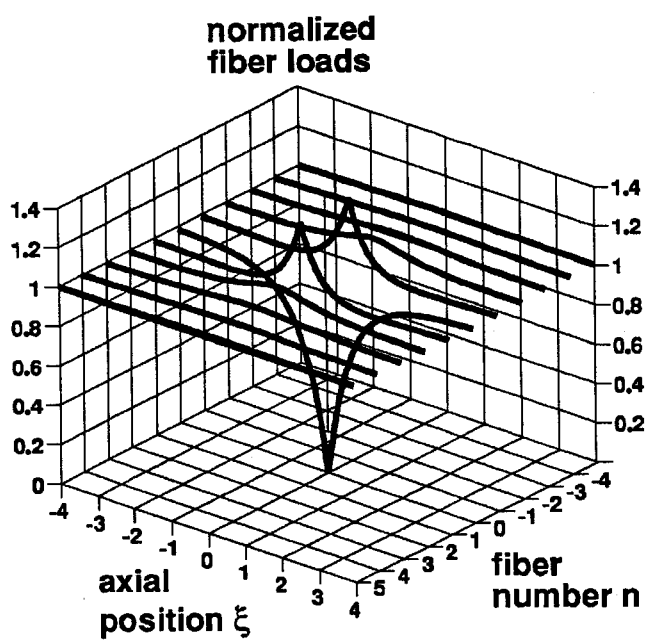

Figure 2. Fiber load profiles in a composite with a single break at (n,ξ) = (0,0), with applied unit edge load at (ξ = ± ∞).

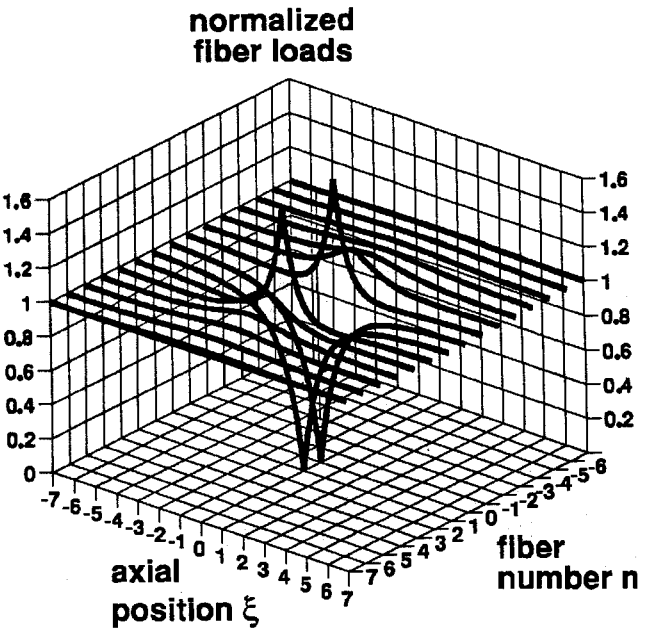

Figure 3. Fiber load profiles in a composite with two breaks, at (n,ξ) = (0,0) and (1,0), with applied unit edge load at (ξ = ± ∞).

These figures demonstrate the magnification, or stress concentration, produced by aligned breaks. It was presumed by Hedgepeth that the failure in a real composite would in all likelihood progress in an orderly fashion at one axial location, where the overloads on fibers neighboring broken fibers would be highest. A single transverse crack would then produce failure. From his mechanical analysis, Hedgepeth (15) inferred the following formula for the stress concentration on the nearest neighboring unbroken fiber, at the same axial location, to n breaks,

$$K_n^{n+1} = \frac{4 \cdot 6 \cdot 8 \cdots (2b+2)}{3 \cdot 5 \cdot 7 \cdot 9 \cdots (2b+1)} \qquad [10]$$

which was later rigorously derived by Hikami and Chou (19) using Legendre polynomials. Inspection of Equation 9, Figure 4b, and comparison of Figures 2, 3, and 5 show that the magnification effect becomes more pronounced as the number of breaks is increased, as one would expect. Figure 5 will shortly be compared with other break patterns in the case of four breaks.

The "spikes" that occur in the load profiles of unbroken fibers adjacent to broken fibers (but not in the other fibers; see Figures 1, 2, and 5) in Figure 4b at $\xi = 0$ are the result of the discontinuity of the fiber at $\xi = 0$. Because the load transfer is accomplished via a fully elastic matrix, the load builds exponentially along the axis of a broken fiber end, with a characteristic shape determined by the ratio of the elastic moduli of the fiber and matrix and the geometry of the composite. The neighboring unbroken fiber is subjected at its center, $\xi = 0$, to shear forces proportional to the derivative of the broken fiber's normal load with axial position. These shear forces acting on the side facing the broken fiber, however, are of opposite sign, for the two adjacent broken fiber ends, which produces the spike in the unbroken fiber's normal load distribution. The

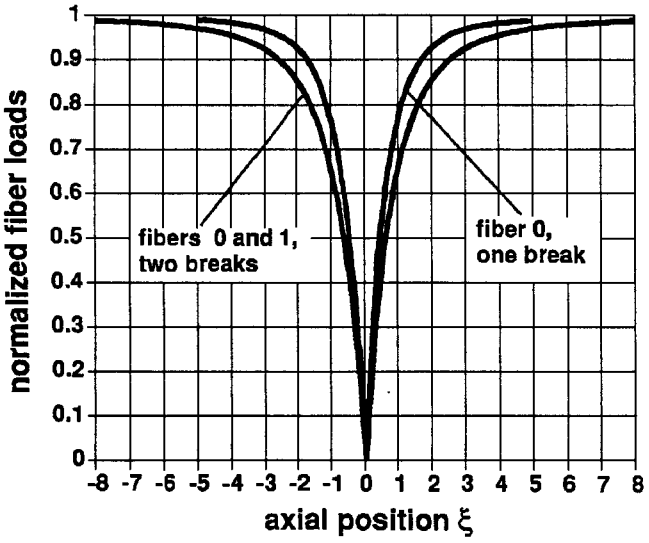

(a)

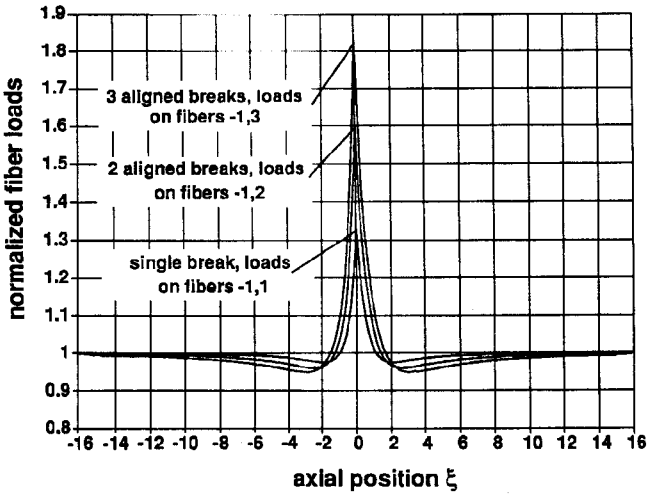

(b)

Figure 4. a) Loads on broken fibers in the case of a single break at (n,ξ) = (0,0), and two breaks at (n,ξ) = (0,0) and (1,0), and b) Loads on unbroken fibers adjacent to broken fibers, showing fiber peak overloads, in three cases: single break at (n,ξ) = (0,0), two breaks at (n,ξ) = (0,0) and (1,0), and three breaks at (n,ξ) = (0,0), (1,0) and (2,0).

sub-adjacent fiber has no such spike since shear is transmitted from an intact fiber, and thus is continuous along the fiber.

SHIELDING OF LOADS WITH MULTIPLE BREAKS

Real composites do not fail along a single, perfect transverse line. Even when tensile failure is observed in a 0° test specimen, and the transverse crack seems rather clean, it is far from perfectly perpendicular to the fibers on the microscopic level. In fact, tiny differences in axial location of sequential fiber breaks create large differences in overload profiles. Because fibers fail at flaws which can be scattered widely, fiber breaks occur at the weakest flaws throughout the composite long before the failure load is reached. A dominant, jagged crack, rather than a single, transversely aligned growing crack causes failure. It is statistically unlikely that the preliminary breaks produced at these low loads will result in failure of the entire composite.

In the case of non-aligned breaks, breaks can actually have an attenuating effect on one another; that is, staggered breaks can actually lessen the severity of the peak overloads in the composite. This "shielding" effect is due to the inability of a broken fiber end to bear much tensile load within some axial distance of its broken end (see Figure 4a, for single and double break examples), and the opposite sign of the shear forces on pairs of broken fiber ends. When break sites are staggered, the load on neighboring unbroken fibers is less than it would be were the breaks aligned because of this effect.

Two simple cases are used to illustrate the effect of this shielding of non-aligned breaks, for the case of four breaks. Referring again to Figure 5, it can be seen that four aligned breaks produce substantial overloads on fibers -1 and 4, which are adjacent to the broken fibers, fibers 0, 1, 2, and 3. The value of the peak stress concentration factor (at fibers -1 and 4 at ξ

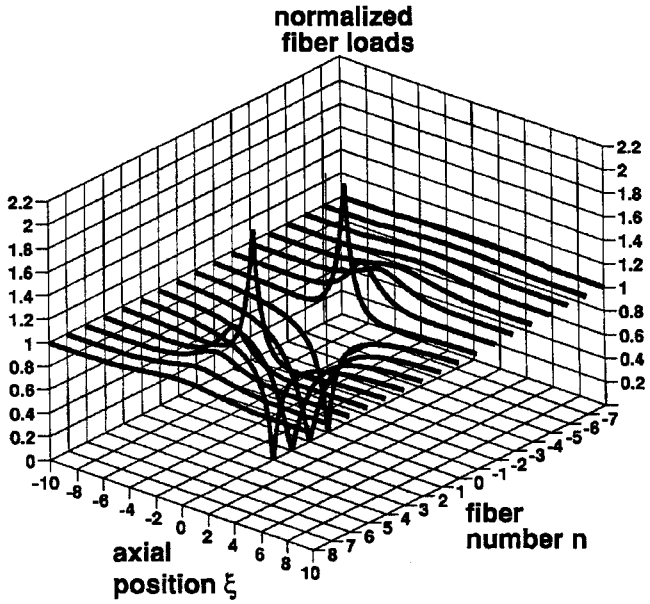

Figure 5. Fiber load profiles in a composite with four breaks, at (n,ξ) = (0,0), (1,0), (2,0) and (3,0), with applied unit edge load at (ξ = ± ∞).

= 0) is 2.032 (see Equation 10). If the locations of the breaks are changed slightly, the resulting overloads are changed dramatically.

Figure 6 shows one possible configuration for four breaks. In fact, in simulations where the fiber elements' strengths are taken into account, this situation arises commonly, and will be the focus of future investigations (20), in that break progressions occur along a jagged lines through the most highly overloaded axial zones for small volumes of composites with high variability in fiber strength. In the case shown in Figure 6, the break "addresses" are (n, ξ) = (0,0), (1,1), (2,0), and (3,1).

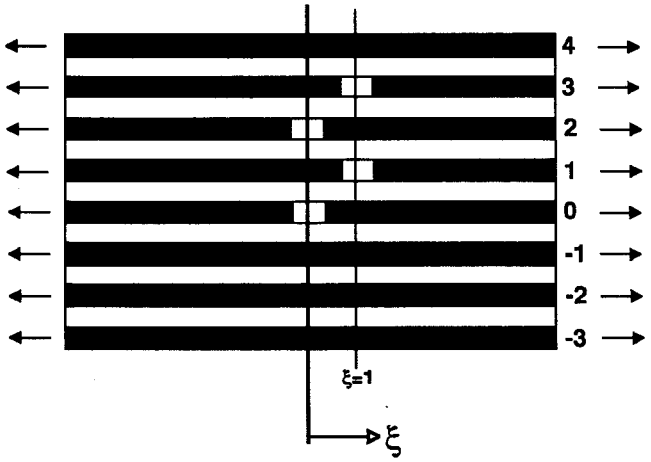

Figure 6. Schematic of a possible break configuration in the case of four breaks, at (n,ξ) = (0,0), (1,1), (2,0), and (3,1).

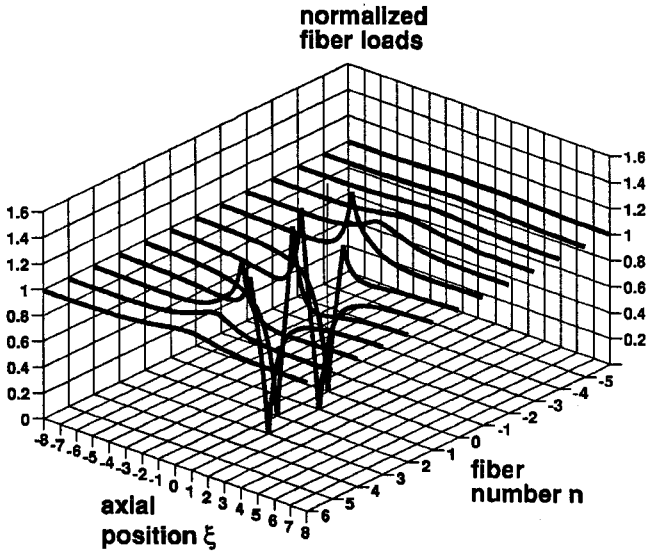

Figure 7. Fiber load profiles in a composite with four staggered breaks, at (n,ξ) = (0,0), (1,1), (2,0), and (3,1), with applied unit edge load at (ξ = ± ∞).

This dimensionless value for the axial break staggering, ξ = 1, corresponds to 10 fiber diameters in the case of a 50% fiber volume fraction composite comprised of fibers and matrix where Ef/Gm = 100 (see Equation 5, with b = d). This misalignment amounts to approximately 100 μm in a typical fiber composite (containing 8-12 μm diameter carbon or Kevlar® fibers). In macroscopic evaluation of a failed tensile specimen, a failure surface containing such slight staggerings of failed fibers would appear to have a reasonably smooth surface.

The resulting load profiles are shown for the case of the four staggered breaks in Figure 7. The shielding effect produced by the staggering of the breaks can be clearly seen on fibers -1 through 4, where the overloads' peaks are substantially less than in the aligned case of Figure 5. Another result of the staggering of the breaks is the presence of peaks in the broken fibers themselves, at the axial location of the adjacent breaks. Figure 8 shows the magnitude of the difference in the peak overloads. In the staggered case, the peak overload is 1.504, at (n,ξ) = (1,0) and (2,1). Thus, in the staggered case, the peak loads have been reduced by about 51%, relative to a unit edge load per fiber, and are located on broken fibers, rather than on unbroken fibers adjacent to broken fibers. The load in unbroken fibers at the adjacent points to the outermost breaks in this situation are 1.441, at (n,ξ) = (-1,0) and (4,1), which is about 57% less than the peak loads in the aligned case relative to a unit edge load per fiber.

Another possible configuration of breaks is shown in Figure 9. The fiber breaks lie at an angle to the axis ξ = 0, at (n,ξ) = (0,0), (1,1), (2,2), and (3,3), with the same axial spacings, although in different directions, of the successive breaks in Figure 7. The shielding effect can be seen on fibers -1 through 4 in Figure 10, with the full load profiles shown in Figure 11. In this case, the peak overload in the composite [at (n,ξ) = (-1,0), and (4,3)] is reduced even further, to 1.372 (approximately 64% less than in the aligned case, relative to a unit edge

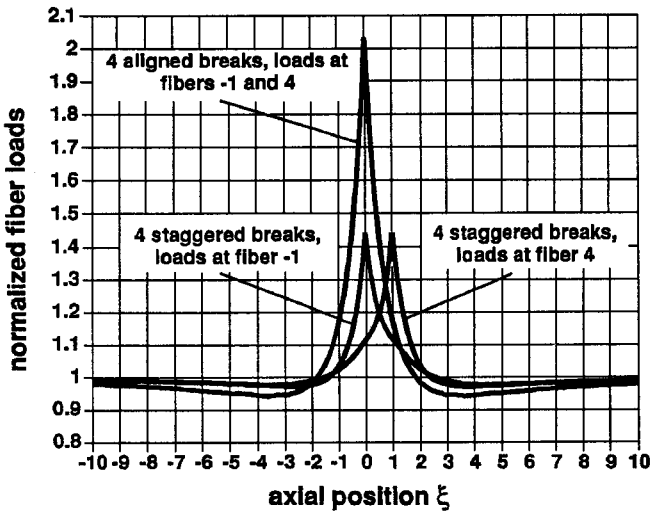

Figure 8. Comparison of the load profiles of the adjacent unbroken fibers to four fiber breaks, for four aligned breaks and four staggered breaks (see Figures 5 and 7 for full load profiles in these cases).

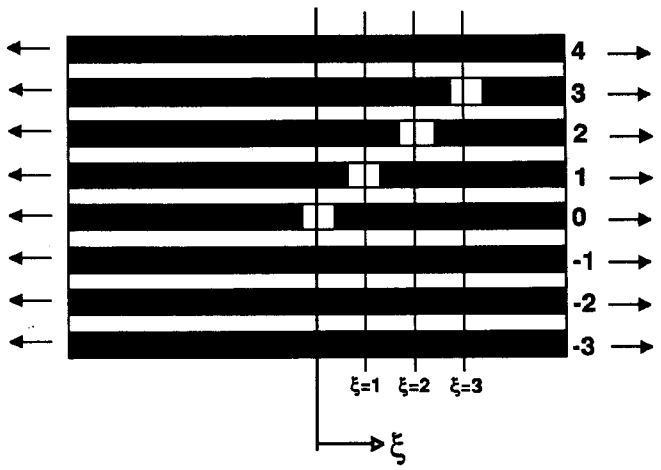

Figure 9. Schematic of another possible break configuration in the case of four breaks, at (n,ξ) = (0,0), (1,1), (2,2), and (3,3).

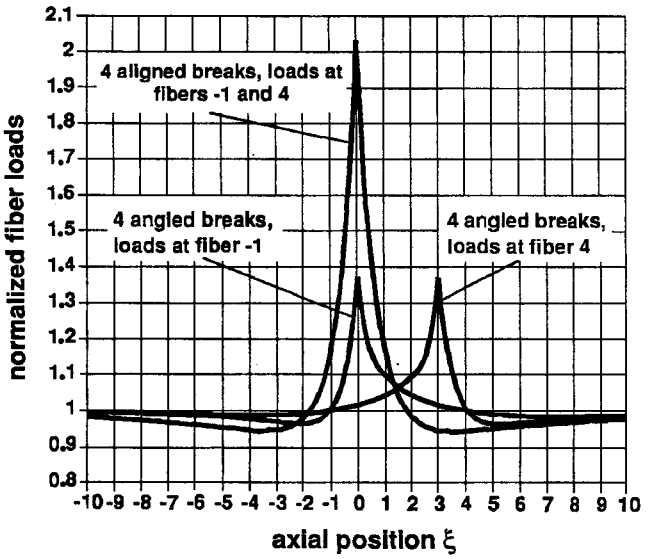

Figure 10. Comparison of the load profiles of the adjacent unbroken fibers to four fiber breaks, for four aligned breaks and four angled breaks (see Figures 5 and 10 for full load profiles in these cases).

load per fiber). This smaller peak load is a result of the wider spacing of the breaks, whose influence on neighboring fibers is reduced with increased axial distance.

THREE-DIMENSIONAL SOLUTIONS

The BIS technique can be used to analyze three-dimensional as well as planar composites containing breaks. Two geometries, shown in Figures 12 and 13 are illustrated here. Figure 12 shows a coordinate system for a square-packed material containing one break, and Figure 13 shows another coordinate

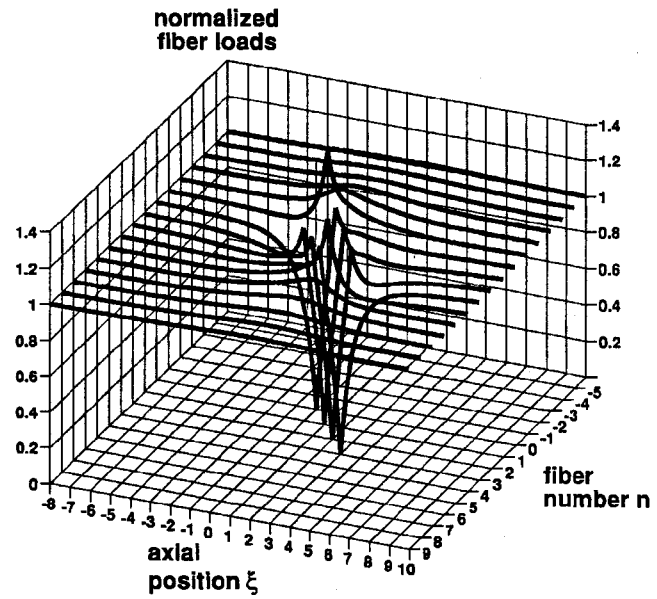

Figure 11. Fiber load profiles in a composite with four angled breaks, at (n,ξ) = (0,0), (1,1), (2,2), and (3,3), with applied unit edge load at (ξ = ± ∞).

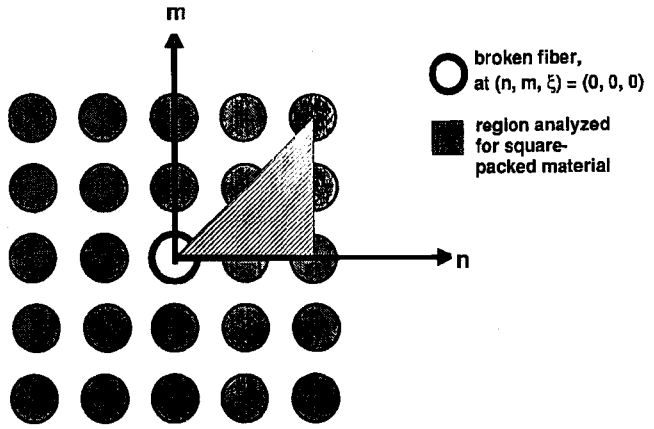

Figure 12. Schematic of coordinate system for the single break problem, in a three-dimensional, square-packed composite.

system for a hexagonally-packed material containing one break. As for the planar case, the single break solution can be used along with boundary conditions such as those in Equation 8 to deduce the resulting load profiles in a material containing arbitrarily located breaks. Hedgepeth and Van Dyke (16) solved for the load profiles in a composite in each of these case, with breaks all contained in the plane $\xi = 0$.

The governing equations for the square and hexagonal cases are respectively

$$\frac{\partial^2 U_n}{\partial \xi^2} + U_{n+1,m} + U_{n,m+1} + U_{n-1,m} + U_{n,m-1} - 4U_{n,m} = 0 \quad [11]$$

and

$$\frac{\partial^2 U_n}{\partial \xi^2} + U_{n+1,m} + U_{n,m+1} + U_{n-1,m} + U_{n,m-1} + U_{n+1,m-1} + U_{n-1,m+1} - 6U_{n,m} = 0 \quad [12]$$

The single-break load profiles, with breaks located at (n,m,ξ) = (0,0,0) (see Figures 12 and 13) can be written compactly as

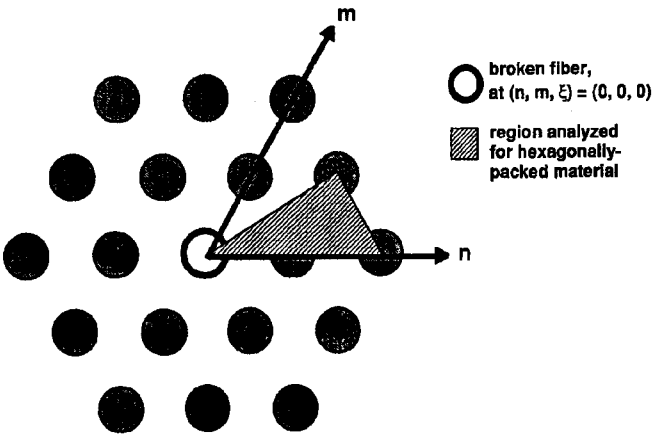

Figure 13. Schematic of coordinate system for the single break problem, in a three-dimensional, hexagonally-packed composite.

$$F_{n,m}(\xi) = \frac{-1}{\int_0^{\pi}\int_0^{\pi} \delta \, d\theta \, d\phi} \qquad [13]$$

$$\int_0^{\pi}\int_0^{\pi} \delta \, e^{-\xi\delta} \cos(n\theta)\cos(m\phi)\, d\theta \, d\phi$$

where the factor δ is given by

$$\delta_s = \sqrt{4 - 2\cos\theta - 2\cos\phi} \qquad [14]$$

and

$$\delta_H = \sqrt{6 - 2\cos\theta - 2\cos\phi - 2\cos\theta\,2\cos\phi} \qquad [15]$$

respectively, for the square- and hexagonally-packed arrays. These solutions give the fiber load profiles for the shifted solution; to obtain the result for an edge unit load with zero load the at the break site, a unit load must be added to Equation 13. The remainder of the analysis follows analogously to the planar case, with (numerical) double integrations replacing the single load integrals for the planar case, as interactions from neighboring fibers in two directions must be considered in the three-dimensional solids.

CONCLUSIONS AND FUTURE WORK

The BIS technique offers a computationally simple method of calculating load profiles in both two-dimensional and three-dimensional, unidirectional, elastic composite. This provides a means of performing strength simulations for large composites using the statistics of fiber strength along with the mechanics of elastic load transfer. While real composites exhibit many types of inelastic behavior which this linear model cannot account for, this technique will provide a means of evaluating current statistical theories against the simplest mechanical case.

Future work will include these strength simulations using both the two- and three- dimensional cases, and suggest scaling techniques for predictions of unidirectional strength.

ACKNOWLEDGMENT

This work was supported by the MRL Program of the National Science Foundation under Award No. DMR-9121654.

REFERENCES

1. A.N. Netravali, R.B. Henstenburg, S.L. Phoenix, and P. Schwartz, *Polymer Composites,* **10,** 226 (1989).
2. A.G. Metcalf and G.K. Schmitz, *ASTM Proceedings,* **64,** 1075 (1964).
3. H.D. Wagner, S.L. Phoenix, and P. Schwartz, *Journal of Composite Materials,* **18,** 312 (1984).
4. K.E. Jackson, S. Kellas, and J. Morton, *Journal of Composite Materials,* **26,** 2674 (1992).
5. C. Zweben, *Composites Technology Review,* **3,** 26 (1981).
6. A.S.Watson and R.L. Smith, *Journal of Materials Science,* **20,** 3,260 (1985).
7. H.E. Daniels, *Proceedings of the Royal Society,* London, Series A, **183,** 405 (1945).
8. L.N. McCartney and R.L. Smith, *Journal of Applied Mechanics,* **105,** 601 (1983).
9. D.G. Harlow and S.L. Phoenix, *Journal of Composite Materials,* **12,** 195 (1978).
10. D.G. Harlow and S.L. Phoenix, *Journal of Composite Materials,* **12,** 314 (1978).
11. S.B. Batdorf, *Journal of Reinforced Plastics and Composites,* **1,** 153 (1982).
12. K. Goda and S.L. Phoenix, to appear in *Composites Science and Technology.*
13. M. Kachanov, "A Simple Technique of Stress Analysis in Elastic Solids with Many Cracks," *International Journal of Fracture,* (Report of Current Research) **23,** R11 (1985).
14. M. Kachanov, *International Journal of Solids and Structures,* **23,** 23 (1987).
15. J.M. Hedgepeth, "Stress Concentrations in Filamentary Structures," NASA Technical Note D-822, May, 1961.
16. J.M. Hedgepeth and P. Van Dyke, *Journal of Composite Materials,* **1,** 294 (1967).
17. W.B. Fichter, Stress Concentrations in Filament-Stiffened Sheets, Ph.D. thesis, Department of Engineering Mechanics, North Carolina State University, 1969.
18. A.M. Sastry and S.L. Phoenix, *Journal of Materials Science Letters,* in press, September, 1993.
19. F. Hikami and T.-W. Chou, *AIAA Journal,* **28,** 499 (1990).
20. A.M. Sastry and S.L. Phoenix, in preparation.

BIOGRAPHIES

Ann Marie Sastry received her Bachelor's Degree in Mechanical Engineering at the University of Delaware in 1989, and is currently completing her Ph.D. in Mechanical Engineering at Cornell University. She received the first place awards at the SAMPE graduate student competitions in 1993 and 1992, in addition to two SAMPE undergraduate awards in 1988 and 1987, and started the SAMPE student chapter. She has accepted a position at Sandia National Laboratories in Albuquerque, New Mexico beginning in February, 1994. Her research areas have included analysis of microcomposite experiments, micromechanics of load transfer, and statistics of composite failure.

Leigh Phoenix received his Bachelor's and Masters Degrees in Agricultural Engineering from the University of Guelph in Canada, and his Ph.D. in Theoretical and Applied Mechanics from Cornell University in 1972. He has been on the faculty at Cornell since 1974 and is currently Professor of Theoretical and Applied Mechanics. In 1983 he won the Fiber Society award for Distinguished Achievement in Basic or Applied Fiber Science and in 1992 he won the ASTM Harold DeWitt Smith Award in recognition of his contribution to the statistical theory of failure of multi-component fiber assemblies. He currently works on statistical theories of failure of composite materials. ♦